Reactive & Functional Polymers 69 (2009) 273–280

Contents lists available at ScienceDirect

Reactive & Functional Polymers

journal homepage: www.elsevier.com/locate/react

Macroporous hydrogel beads of high toughness and superfast responsivity

Fuat Topuz, Oguz Okay *

Istanbul Technical University, Department of Chemistry, 34469 Maslak, Istanbul, Turkey

ARTICLE INFO

Article history:
Received 22 November 2008
Received in revised form 12 January 2009
Accepted 19 January 2009
Available online 24 January 2009

Keywords:
Hydrogel beads
Macroporous
Cryogelation
Elasticity

ABSTRACT

Macroporous hydrogel beads based on the monomers acrylamide and 2-acrylamido-2-methylpropane sulfonic acid sodium salt were prepared by dropwise addition of the monomer solution into the paraffin oil as the continuous phase at subzero temperatures. The beads prepared between −15 and −20 °C have irregular large pores of 1–10 μm in diameter, typical for macroporous networks created by the cryogelation technique, while nonporous hydrogels were obtained at room temperature. Swelling measurements show that the low temperature beads swell within seconds to attain their equilibrium states in water. The beads formed at subzero temperatures were very tough and can be compressed up to 94% strain without any crack development while those formed at room temperature were fragile and broke at a strain of about 40%. The results indicate that the tough hydrogel beads formed at subzero temperatures can be used in separation processes in which the separated compounds can easily be recovered by compression of the beads under a piston.

1. Introduction

Responsive hydrogels are smart and soft materials, capable of changing volume in response to specific external stimuli, such as the temperature, solvent quality, pH, and electric field [1,2]. These properties of hydrogels received considerable interest in last three decades and, a large number of hydrogel based devices have been proposed, including drug delivery systems, artificial organs, actuators, and on–off switches [3,4]. However, the practical design and control of these devices still present some problems. For example, although a fast response rate of hydrogels is a requirement in many application areas, hydrogels are limited in their response rate by diffusion processes, which are slow and even slower near the critical point [5]. Moreover, the durability of the hydrogel based devices requires a good mechanical performance of gels in their swollen state. Polymer gels under interest are, however, soft and fragile when handled in the swollen state. The poor mechanical performance of highly swollen hydrogels limits their technological applications.

Recently, we have shown that by conducting the free-radical crosslinking copolymerization reactions below the freezing point of the gelation system, macroporous gels based on acrylamide (AAm) as well as 2-acrylamido-2-methylpropane sulfonic acid sodium salt (AMPS) monomers with superfast swelling properties could be obtained [6–8]. This was achieved by using gelation reactions occurring in the apparently frozen reaction system, which allowed for the formation of a bicontinuous morphology in polymer networks [9–13]. It was shown that the free water freezing in the gel causes the network chains to gather and condense so that a heterogeneous network forms after removing the ice. The polymer network maintains a honeycomb structure upon drying. Further, the hydrogels prepared from frozen solutions were very tough and, they can be compressed without any crack development [8,13]. This behavior of macroporous hydrogels formed by low temperature gelation is advantageous compared to those obtained by phase separation mechanism where materials with poor mechanical performance were obtained [14].

Here, we describe the preparation of macroporous hydrogels of high toughness and superfast responsivity in the form of millimeter-sized beads. Hydrogel beads have attracted attention as carrier matrices in a wide variety of medical and biological applications, such as affinity chromatography, immobilization technologies, and drug delivery systems [2]. In the present work, the aqueous phase crosslinking reactions of AAm monomer and AMPS ionic comonomer were carried out at subzero temperatures in paraffin oil as the continuous phase. The beads obtained were characterized by swelling and elasticity tests. It should be pointed out that, although significant progress has been made towards structural characterization of cylindrical gel samples, much less has been published about their characterization in the form of spheres. For uniaxial compression of a cylindrical gel sample, the statistical theories of rubber elasticity yield for Gaussian chains an equation of the form [15,16]:

$$f = G(\alpha - \alpha^{-2}) \tag{1}$$

where f is the stress, α is the corresponding deformation ratio (deformed length/initial length) and G is the elastic modulus of the

---

* Corresponding author. Tel.: +90 212 2853156; fax: +90 212 2856386.
E-mail address: okayo@itu.edu.tr (O. Okay).

1381-5148/$ - see front matter © 2009 Elsevier Ltd. All rights reserved.
doi:10.1016/j.reactfunctpolym.2009.01.009

sample. In contrast to a cylindrical gel sample, the interpretation of the compression test data of a spherical gel particle is complicated. This is due to the significant variation of the contact area between the wall and the originally spherical gel during deformation. For a sphere with a constant volume during deformation, Hertz derived the following equation for small deformation ranges [17–21]:

$$F = \frac{4}{3} G D^{0.5} \Delta D^{1.5} \qquad (2)$$

where F is the force and ΔD is the deformation, $\Delta D = D - D'$, D and D' are the initial undeformed and deformed diameters of the sample, respectively. Only a few works have been reported on the mechanical measurements of individual gel beads [18,22–24]. Here, we also report the results of the elasticity tests conducted on individual hydrogel beads formed at various temperatures.

2. Experimental

2.1. Materials

Acrylamide (AAm, Merck), N,N′-methylenebis(acrylamide) (BAAm, Merck), ammonium persulfate (APS, Fluka), N,N,N′,N′-tetramethylethylenediamine (TEMED, Merck), and paraffin oil (Riedel de Haen) were used as received. 2-Acrylamido-2-methylpropane sulfonic acid (AMPS-H$^+$, Merck) was neutralized with NaOH and a stock solution was prepared containing 0.966 M AMPS. Stock solutions of BAAm and APS were prepared by dissolving 0.130 g BAAm and 0.205 g APS each in 10 mL of distilled water.

2.2. Preparation of macroporous beads

Macroporous poly(AAm-co-AMPS) hydrogel beads were prepared by conducting the aqueous phase crosslinking copolymerization of AAm and AMPS monomers with BAAm crosslinker at subzero temperatures within the millimeter-sized droplets. Paraffin oil was used as the continuous phase. The synthesis parameters were fixed as follows:

Monomer concentration in the aqueous phase = 9.5 w/v%
Crosslinker ratio = 1 mol BAAm/83 mol AAm + AMPS
Ionic group content = 0.40 mol AMPS/mol AAm + AMPS
APS concentration in the aqueous phase = 9.0 mM
TEMED concentration = 0.60 mL/100 mL aqueous phase

Typically, AAm (0.301 g), water (5 mL), and stock solutions of AMPS (2.90 mL) and BAAm (1.00 mL) were mixed in a glass vial. After bubbling nitrogen for 10 min, TEMED (0.060 mL) and APS stock solution (1.00 mL) were added. Separately, a glass jar containing 200 mL of paraffin oil was immersed in a cryostat at the polymerization temperature T_{prep}. The decrease of the temperature of the paraffin oil was monitored by a thermocouple immersed in the oil bath. As long as the oil temperature reaches to −4 °C, the aqueous solution was added dropwise using micropipettes of various tip diameters into the paraffin oil within one minute. Fig. 1 shows the cooling profile of the oil phase for experiments conducted at various temperatures T_{prep} and the time of addition of the monomer phase. After three days, the gel beads were removed from the oil phase, washed several times with acetone and then dried in a vacuum at room temperature. Thereafter, they were placed in an excess of water and water was replaced many times.

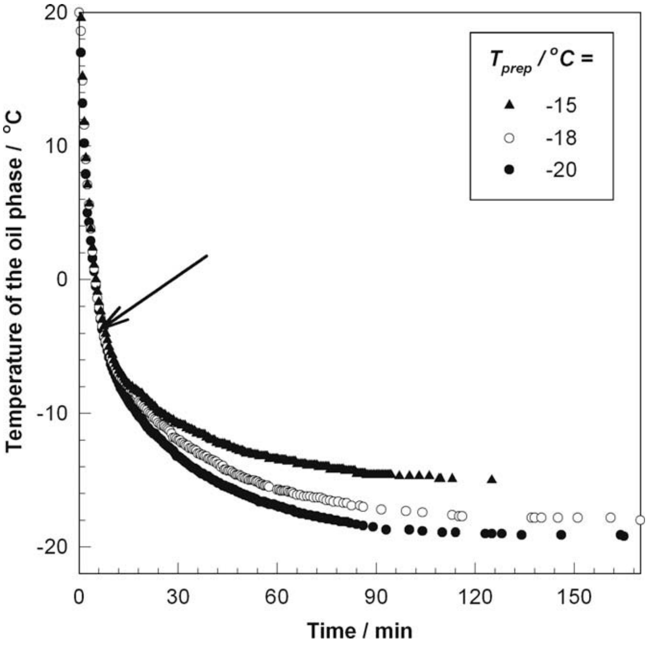

Fig. 1. Cooling profile of the continuous phase for various T_{prep}. The arrow shows the time of the addition of the aqueous phase.

We should note that the procedure detailed above was obtained after several preliminary experiments conducted under various experimental conditions. For example, odd-shaped hydrogel particles were obtained if the reactions were carried out under continuous stirring of the oil phase, probably due to the collisions between the frozen particles. Moreover, at low stirring rates, agglomerates of hydrogel particles were obtained. Addition of the aqueous phase into the oil phase before cooling resulted in nonporous hydrogels. Further, if the oil phase is cooled down to the polymerization temperature T_{prep} before the addition of the aqueous phase, the added droplets remained on the oil surface due to the increased density of the oil phase so that no particles could be obtained. To obtain macroporous beads with a high degree of sphericity, −4 °C was determined to be the optimum temperature for the addition of the droplets into the oil phase.

2.3. Preparation of nonporous beads

For comparison, hydrogel beads were prepared under the same condition as above except that the temperature of the oil phase was set to 19 °C and it was stirred during the reactions. For this purpose, the reactions were conducted in a 1 L round-bottom, four-neck reactor, fitted with a mechanical stirrer, nitrogen inlet, condenser, and pipette outlet. 400 mL of paraffin oil were first introduced to the reactor and stirred at 100 rpm under nitrogen atmosphere at 19 °C. Then, 40 mL of an aqueous monomer solution of AAm (1.2036 g), BAAm (0.0520 g), APS (0.0820 g) and AMPS stock solution (11.6 mL) were transferred into the reactor. After 1 min, TEMED (0.24 ml.) was added to the mixture to initiate the polymerization. The reactions proceeded for 3 h at 19 °C. At the end of the polymerization, the gel beads were removed from the oil phase, and treated with acetone and water as described above.

2.4. Swelling measurements

Swelling measurements were conducted on individual hydrogel beads equilibrium swollen in water. The swelling data were obtained using beads of various swollen diameters between 4.5 and 8.6 mm. The beads were placed separately in glass vials containing an excess of water at 21 ± 0.5 °C. In order to reach swelling equilibrium, the beads were immersed in water for at least two weeks replacing the water many times. The swelling equilibrium was tested by measuring the diameter of the gel beads by using an im-

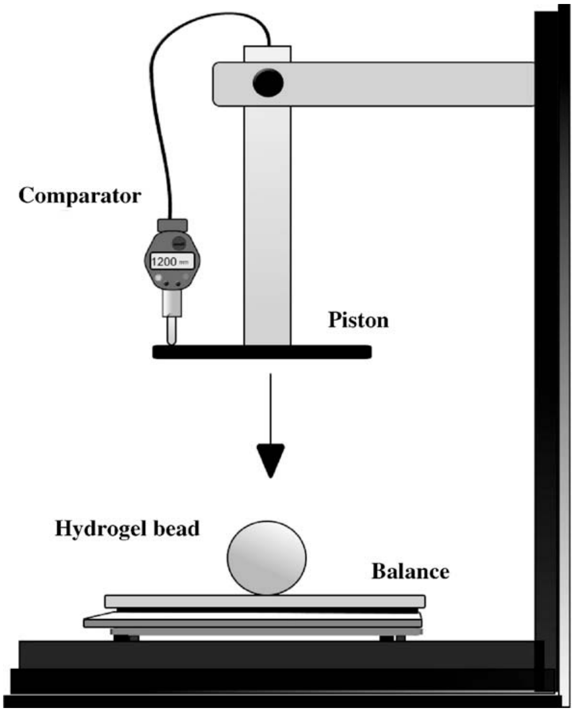

Fig. 2. Uniaxial compression apparatus for measuring stress–strain data on hydrogel beads.

age analyzing system consisting of a microscope (XSZ single zoom microscope), a CDD digital camera (TK 1381 EG) and a PC with the data analyzing system Image-Pro Plus. The swelling equilibrium was also tested by weighing the gel beads. For this purpose, the gel bead was taken out of water and left on a dry plastic surface for 1 min. Since touching a filter paper to the surface of the bead removed water from the gel phase, the bead was carefully taken from the surface using a dry spoon and then weighed on a digital balance (Precisa Series 320 XB, Model 220A, readability and reproducibility = 0.1 mg). Thereafter, the hydrogel beads equilibrium swollen in water were dried in a freeze dryer to constant weight. The equilibrium volume and the equilibrium weight swelling ratios of the beads, q_v and q_w, respectively, were calculated as:

$$q_v = (D/D_{dry})^3 \tag{3}$$

$$q_w = m/m_{dry} \tag{4}$$

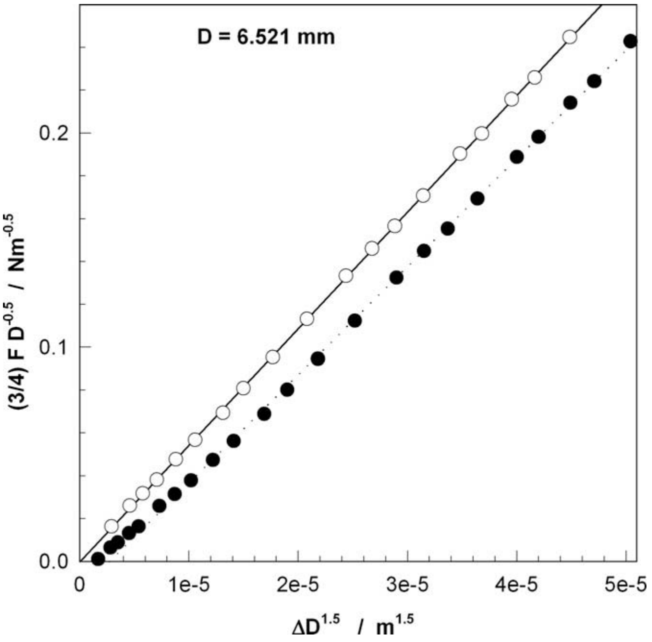

Fig. 3. Typical stress–strain data for a hydrogel bead prepared at 19 °C. (●) Uncorrected data; (○) corrected data.

where D and D_{dry} are the diameters of the equilibrium swollen and dry beads, respectively, m and m_{dry} are the weights of beads after equilibrium swelling in water and after drying, respectively. Note that the swelling measurements were conducted on at least six individual beads prepared under the same experimental condition and the results were averaged. The masses of dry beads were between 1.3 and 4.1 mg, i.e., within the accuracy level of the balance used.

For the measurement of the deswelling rates of gel beads, the equilibrium swollen hydrogel beads in water were immersed in acetone at 21 °C. The volume changes of beads were measured in-situ by following the diameter of the samples under microscope using the image analyzing system. For the measurement of the swelling rates of beads, the collapsed gel beads in acetone were transferred into water at 21 °C. The diameter changes of the beads were also determined as described above.

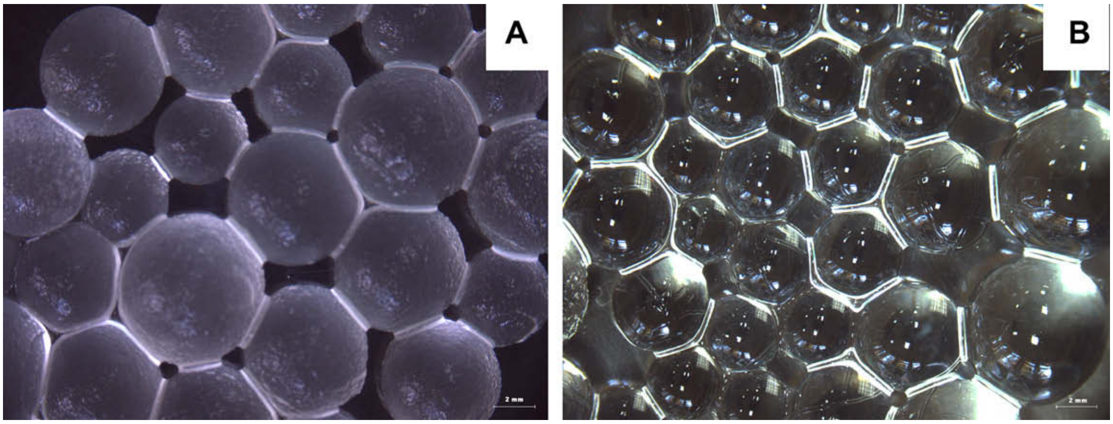

Fig. 4. Optical images of hydrogel beads formed at −18 °C (A) and 19 °C (B). Scaling bar = 2 mm.

2.5. Elasticity tests

Uniaxial compression measurements were performed on individual hydrogel beads in their swollen states. All the mechanical measurements were conducted in a thermostated room of 21 ± 0.5 °C. The key parts of the apparatus used are shown in Fig. 2.

Briefly, a gel bead of 3–13 mm in diameter was placed on a digital balance (Precisa 320 XB-220A, readability and reproducibility = 0.1 mg). A load was transmitted vertically to the gel through a rod fitted with a PTFE end-plate. The force F acting on the gel was calculated from the reading of the balance m as $F = mg$, where g is the gravitational acceleration. The resulting deformation ΔD was measured using a digital comparator (IDC type Digimatic Indicator 543-262, Mitutoyo Co.), which was sensitive to displacements of 10^{-3} mm. The force and the resulting deformation were recorded after 20 s of relaxation. During the measurements, the load increment in successive steps was so adjusted that the gel bead was deformed 50–60 μm in each step. The measurements were conducted up to about 20% compression.

Table 1
Characteristics of the hydrogel beads prepared at various temperatures T_{prep}. The numbers in parenthesis are the standard deviations of at least six measurements. q_w, weight swelling ratio; q_v, volume swelling ratio; P_s, swollen state porosity; V_p, total pore volume; G, elastic modulus of the bead in swollen state. The data were obtained using beads of various swollen diameters between 4.5 and 8.6 mm in the swelling tests, and 3–11 mm in the elasticity tests.

T_{prep}/°C	q_w	q_v	P_s %	V_p/mL g^{-1}	G/kPa
19	120 (24)	135 (22)	0	0.1 (0.1)	5.2 (1.3)
−15	60 (3)	26 (3)	68 (4)	3.9 (1)	2.6 (0.3)
−18	63 (4)	33 (3)	61 (8)	3.5 (0.8)	2.4 (0.3)
−20	90 (6)	44 (10)	64 (18)	4.6 (0.3)	2.5 (0.6)

We first conducted the compression measurements on individual gel beads immersed in a large excess of water. However, no reproducible results were obtained from these measurements, probably due to the motion of the bead during compression. Measurements conducted outside of the water phase gave reproducible results. The weight loss of single beads during the measurement due to water evaporation or due to the applied force was found to be negligible. This was achieved by keeping the measurement time as short as possible. One measurement took only less than 10 min involving 10–30 data points.

According to Eq. (2), a linear relation was expected if $(3/4)FD^{-0.5}$ is plotted against $\Delta D^{1.5}$ with a slope equals to the modulus G of the beads. A typical plot is given in Fig. 3 for a hydrogel bead formed at 19 °C. A discrepancy from the linear relationship is obvious at small compressions, which was observed in all gel beads prepared in this study. This deviation from theory can be attributed to the imperfect geometry of the surface of the bead, which decreases the contact area between the PTFE plate and the sample at low compression, and results in relatively high deformations at low stresses. In order to correct this imperfection, the isotherm was re-drawn by discarding the data at very low strains. The linear portion of the curve was then extrapolated to a value of $\Delta D^{1.5}$ at $F = 0$ (dashed curve in Fig. 3) from which the corrected initial diameter was computed and the deformation ratios were suitably adjusted. The data corrected in this manner are also shown in Fig. 3 as open

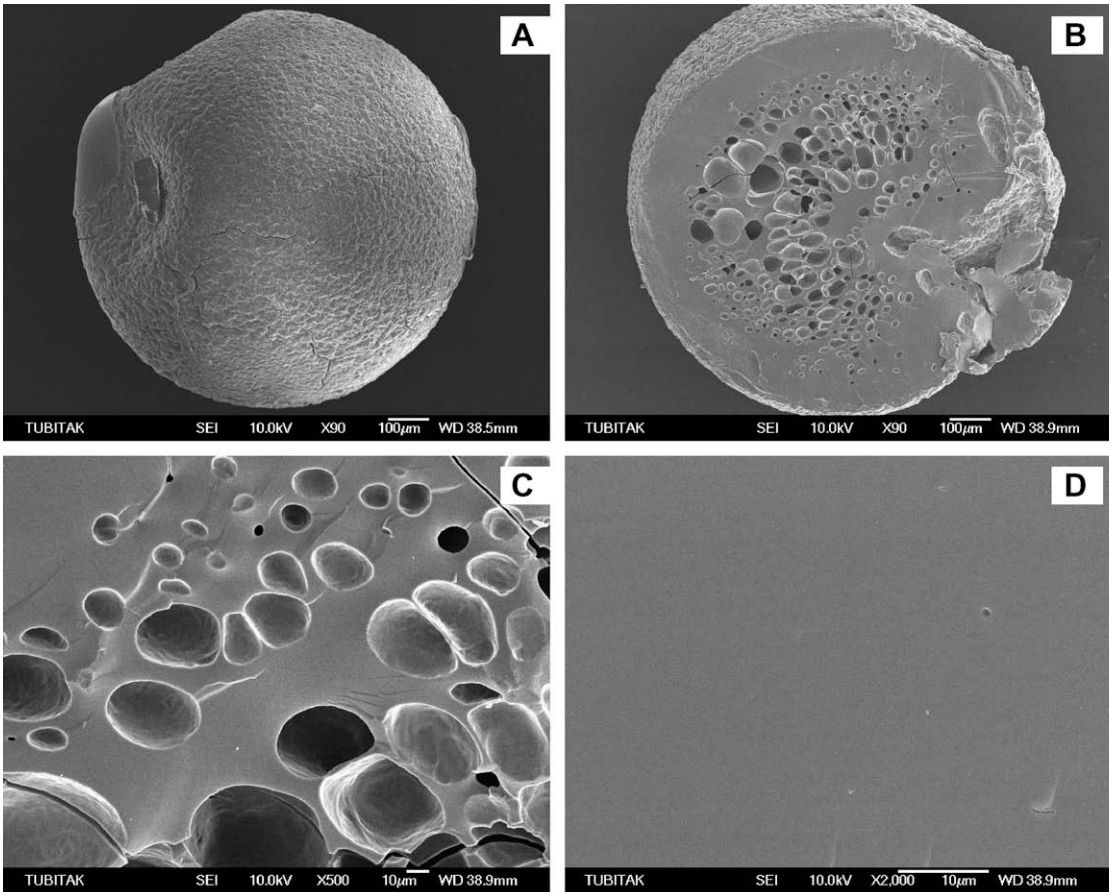

Fig. 5. SEM of the bead networks formed at T_{prep} = 19 °C. The scaling bars are 100 μm (A and B), and 10 μm (C and D). Pictures C and D were taken from the inner and outer parts of the bead, respectively.

symbols. The reversibility of the gel deformation was also checked by several samples and found to be reversible. From the repeated measurements, the standard deviations in the modulus value were less than 3%.

2.6. Texture determination and porosity of beads

For the texture determination of freeze-dried hydrogel beads, scanning electron microscopy (SEM) studies were carried out at various magnifications between 50 and 2000 times (Jeol JSM 6335F Field Emission SEM). Prior to the measurements, network samples were sputter-coated with gold for 3 min using Sputter-coater S150B Edwards instrument.

The pore volume V_p of the beads was estimated through uptake of methanol of dry beads. Since methanol is a nonsolvent for the polymer, it only enters into the pores of the polymer networks. Thus, V_p (mL pores in one gram of dry polymer network) was calculated as,

$$V_p = (m_M - m_{dry})/(d_M \; m_{dry}) \tag{5}$$

where m_M is the weight of the bead immersed in methanol after 3 h and d_M is the density of methanol (0.792 g/mL).

3. Results and discussion

Spherical and monodisperse porous beads of diameters between 2 and 14 mm were prepared by dropwise addition of the monomer solution into the paraffin oil as the continuous phase. The diameter of the porous beads could be adjusted by changing the tip diameter of the pipettes from which the aqueous phase was added into the oil phase. Fig. 4 shows typical pictures of the hydrogel beads prepared at −18 and 19 °C. The beads formed at 19 °C were transparent while those obtained at subzero temperatures were opaque indicating the heterogeneity of the gel network.

Swelling, elasticity, and porosity characteristics of the beads were collected in Table 1 together with the standard deviations given in the parenthesis. All the measurements were conducted on individual hydrogel beads. It is seen that both the weight q_w and the volume swelling ratios q_v of beads formed at subzero temperatures are much smaller than the hydrogel beads formed at 19 °C. This is a consequence of the gelation reactions occurring in frozen solutions; reactions only proceed in the unfrozen domains having a high monomer and crosslinker concentration so that the resulting gels exhibit a lesser degree of swelling as compared to the homogeneous gels [6,7].

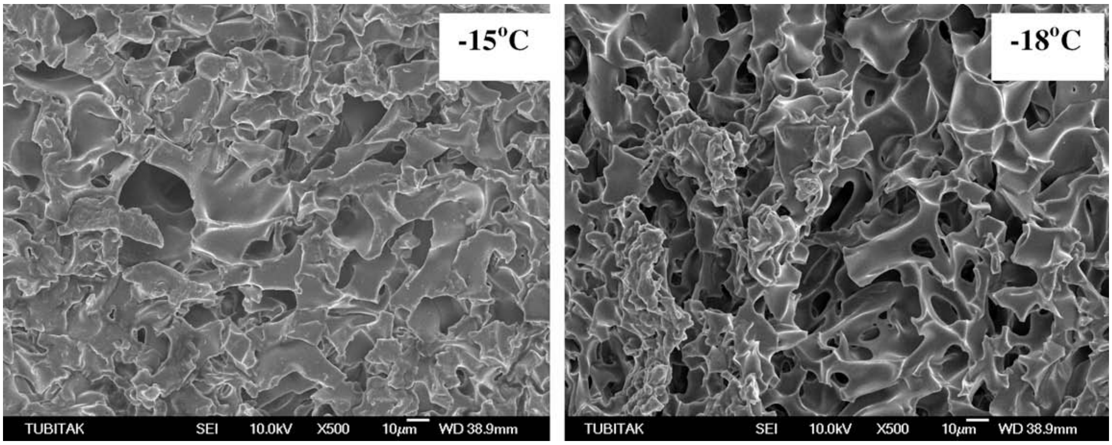

Fig. 6. SEM of the bead networks formed at $T_{prep} = -15$ and -18 °C. The scaling bar is 10 µm. Magnification = 500×.

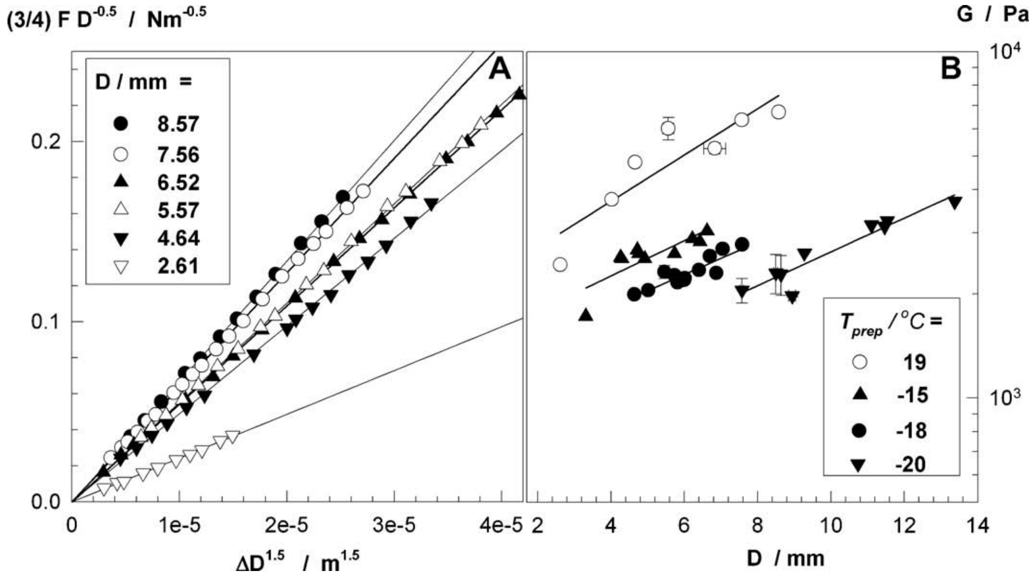

Fig. 7. (A) Stress–strain data for hydrogel beads prepared at 19 °C. Swollen bead diameters *D* are indicated. (B) The elastic modulus *G* of swollen beads as function of their diameters *D* for gels prepared at various temperatures T_{prep}.

The weight swelling ratio q_w of a porous gel represents the amount of the solvent locating in both pores and in the polymer region. In contrast, however, assuming isotropic swelling, the volume swelling ratio q_v represents the amount of the solvent only in the polymer region. Thus, the larger the difference between q_w and q_v, the larger the amount of solvent in the pores, i.e., the larger the total volume of pores. From the q_w and q_v of gels, their swollen state porosities P_s can be estimated as [14]:

$$P_s\,\% = \left(1 - \frac{q_v}{1 + (q_w - 1)\,d_2/d_1}\right) \times 10^2 \tag{6}$$

where d_1 and d_2 are the densities of the solvent (water) and the polymer, respectively. Assuming $d_1 = 1.0$ g/mL and $d_2 = 1.35$ g/mL [25], the swollen state porosities P_s were calculated and are shown in Table 1. The gel beads formed at 19 °C are nonporous while those formed at subzero temperature exhibit more than 60% porosities in their swollen states. Further, P_s does not change much with decreasing preparation temperature from −15 to −20 °C. Similar results were also obtained from the porosity measurements conducted using methanol uptake tests of the individual beads. The results given in Table 1 reveal that the total volume V_p of the pores is about 4 mL/g for all the low temperature gel beads while those formed at 19 °C exhibit negligible porosities.

To visualize the pores in the gel beads, the freeze-dried bead samples were investigated by scanning electron microscopy (SEM). Figs. 5 and 6 show SEM images of the network samples formed at 19 °C and at subzero temperatures, respectively. It is seen that the outer surface layer of the bead formed at 19 °C is nonporous while the inner part consists of large, closed pores which are not interconnected. The existence of closed pores in such hydrogel beads is probably due to the paraffin oil trapped within the monomer droplets during the inverse suspension polymerization. Moreover, in accord with the porosity results, the beads prepared at subzero temperatures have a porous structure with irregular large pores of 1–10 μm in diameter, typical for macroporous networks created by the cryogelation technique (Fig. 6) [6,7].

Elasticity measurements were conducted by the compression tests on individual beads swollen in water. Typical stress–strain curves in the form of $(3/4)FD^{-0.5}$ versus $\Delta D^{1.5}$ plots for hydrogels prepared at 19 °C are shown in Fig. 7A. The data were obtained using beads of various diameters between 2.6 and 8.6 mm. It is seen that the slopes of the regression lines corresponding to the elastic moduli G of the hydrogels vary depending on the bead diameter. Similar plots were also observed using the low temperature gel beads. In Fig. 7B, the moduli of elasticity G of the beads formed at various temperatures are plotted against the bead diameter D. The general trend is that the elastic modulus G, i.e., the average effective crosslink density of the bead increases with increasing bead diameter or, with increasing preparation temperature T_{prep}. The size dependent crosslink density of the hydrogel beads may be connected with the suspension polymerization technique [24,26]. During gelation, the reactions at the surface layer of the monomer droplets are expected to slow down due to the contact of this region with the continuous oil phase. This will reduce

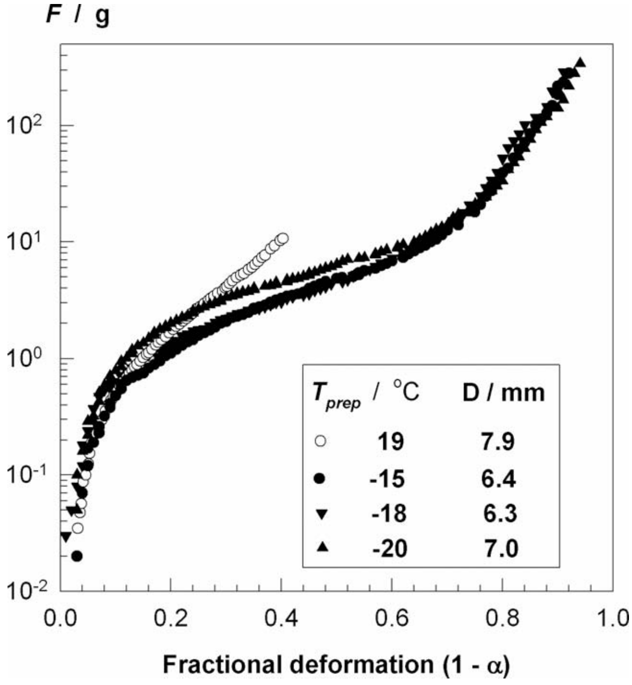

Fig. 9. Stress–strain data of the hydrogel beads prepared at various temperatures T_{prep} as the dependence of the force F on fractional deformation 1-α of beads. The diameters of the hydrogel beads subjected to the mechanical tests are indicated.

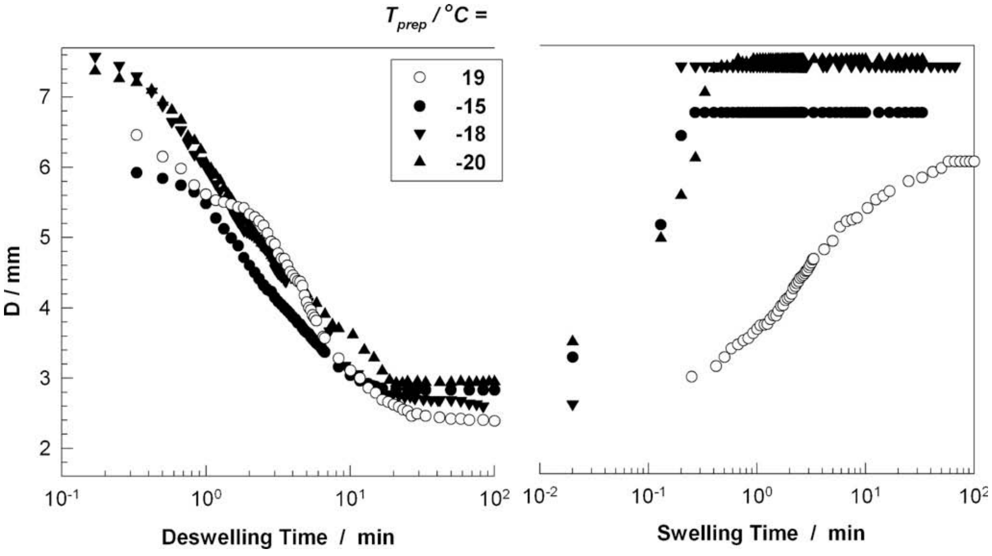

Fig. 8. Diameter D of hydrogel beads shown as a function of the time of deswelling in acetone and re-swelling in water. T_{prep} is indicated.

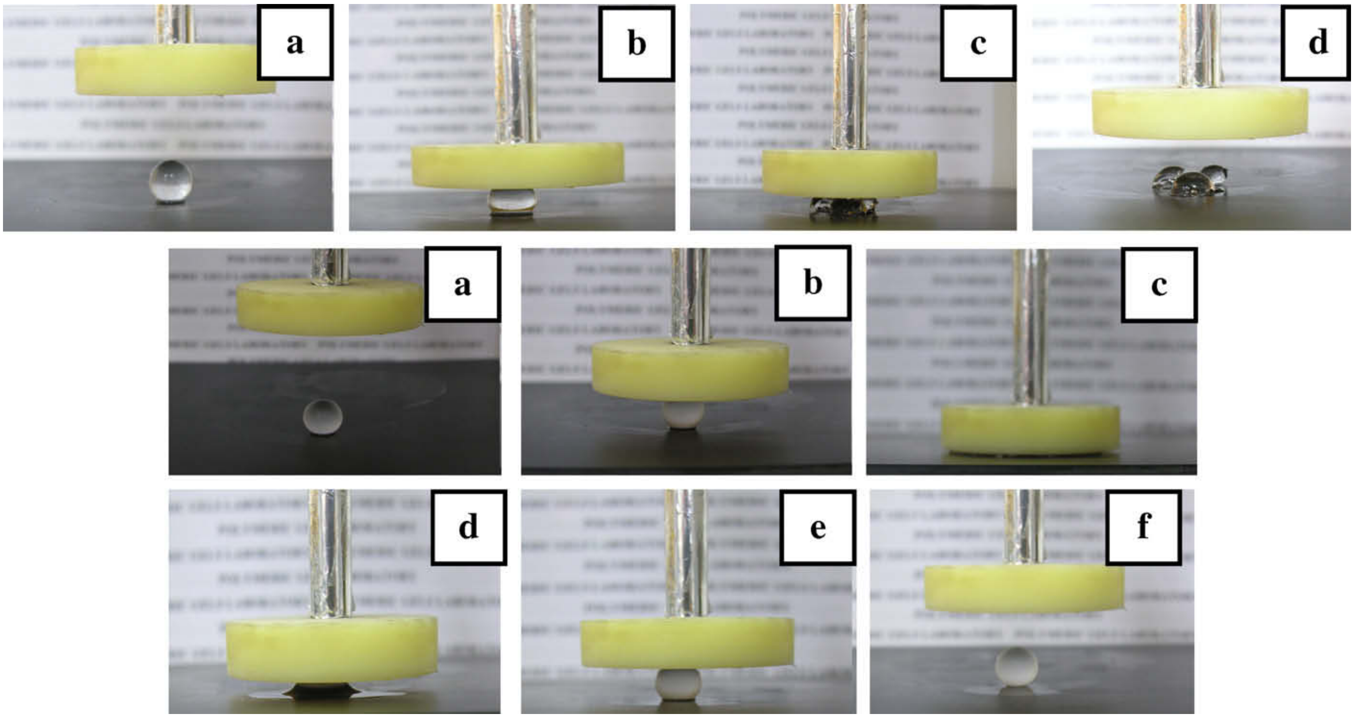

Fig. 10. Photographs of the hydrogel beads formed at $T_{prep} = 19\ ^\circ\mathrm{C}$ (upper panel) and $-18\ ^\circ\mathrm{C}$ (bottom panel) during the compression tests.

the crosslinking density of the surface layer of the resulting gel beads. Since decreasing size of the monomer droplets increases surface-to-volume ratio of the final beads, the smaller the bead diameter, the smaller its average crosslink density. The average values of the modulus of the beads collected in the last column of Table 1 show that the modulus of low temperature beads is about 2.5 kPa compared to 5.2 kPa for beads formed at 19 °C. Decreasing modulus by decreasing temperature is due to the decreasing rate of crosslinking reactions at subzero temperatures.

Fig. 8 compares the response rate of the hydrogel beads prepared at various temperatures T_{prep}. Here, the diameter D of the beads monitored by real-time measurements is plotted against the time t of deswelling in acetone and re-swelling in water. The deswelling rate of the beads does not change much with T_{prep}; all the beads assume a collapsed conformation in acetone within 20 min. In contrast, however, the swelling of the collapsed beads formed at subzero temperatures occurs much faster than the conventional beads formed at 19 °C. The low temperature gel beads attain their equilibrium swollen states within 20 s, while the conventional bead requires 100 min to attain the equilibrium state in water. Since formation of a porous structure increases the response rate of gels, the results are in accord with the microscopic observation of the network structures reported above.

Although the gel beads prepared at a low temperature exhibit a low modulus of elasticity (Table 1), they were very tough and can be compressed up to about 100% strain without any crack development. This behavior is shown in Fig. 9 where the force acting on the bead F is plotted against the fractional deformation $(1-\alpha)$ for gels formed at various T_{prep}. The hydrogel beads prepared at room temperature broke at a stress of about 10 g and a strain of about 40%. However, all the low temperature beads did not break even at a strain of about 94%. Photographs in Fig. 10 also demonstrate how the low temperature gel beads sustain a high compression. As shown in the upper panel of Fig. 10, the swollen bead prepared at room temperature fractured under low deformation suggesting that cracks develop easily in the gel. However, those obtained at a low temperature remain mechanically stable up to about complete compression (bottom panel of Fig. 10). Important point is that, as the low temperature bead is squeezed under the piston, the gel releases all its water so that it can completely be compressed. After the release of the load and, after addition of water, the sample immediately recovers its original shape, as shown in Fig. 10.

4. Conclusions

Free-radical crosslinking copolymerization of AAm and AMPS in the presence of BAAm crosslinker was carried out in aqueous solutions at various temperatures. To obtain spherical macroporous beads, the aqueous monomer solution was added dropwise into the paraffin oil and the reactions were conducted between −15 and −20 °C. For comparison, hydrogel beads were also prepared at 19 °C using inverse suspension polymerization technique. The beads prepared at subzero temperatures have irregular large pores of 1–10 μm in diameter, typical for macroporous networks created by the cryogelation technique. Swelling measurements show that the low temperature beads swell within seconds to attain their equilibrium states in water. The beads formed at low temperatures were very tough and can be compressed up to 94% strain without any crack development while those formed at room temperature were fragile and broke at a strain of about 40%. The results thus indicate that tough hydrogel beads formed at subzero temperatures can be used in separation processes in which the separated compounds can easily be recovered by compression of the beads under a piston.

References

[1] M. Shibayama, T. Tanaka, Adv. Polym. Sci. 109 (1993) 1.
[2] I. Galaev, B. Mattiasson, Smart Polymers: Applications in Biotechnology and Biomedicine, CRC Press, Boca Raton, FL, 2008.
[3] M. Suzuki, O. Hirasa, Adv. Polym. Sci. 110 (1993) 241.
[4] C. Santulli, S.I. Patel, G. Jeronimidis, F.J. Davis, G.R. Mitchell, Smart. Mater. Struct. 14 (2005) 434.
[5] T. Tanaka, D.J. Fillmore, J. Chem. Phys. 70 (1979) 1214.

[6] M.M. Ozmen, O. Okay, Polymer 46 (2005) 8119.
[7] M.V. Dinu, M.M. Ozmen, E.S. Dragan, O. Okay, Polymer 48 (2007) 195.
[8] M.M. Ozmen, O. Okay, React. Funct. Polym. 68 (2008) 1467.
[9] V.I. Lozinsky, Russ. Chem. Rev. 71 (2002) 489.
[10] F. Plieva, X. Huiting, I.Yu. Galaev, B. Bergenstahl, B. Mattiasson, J. Mater. Sci. 16 (2006) 4065.
[11] F.M. Plieva, M. Karlsson, M.R. Aguilar, D. Gomez, S. Mikhalovsky, I.Yu. Galaev, Soft Matter 1 (2005) 303.
[12] G.A. Komarova, S.G. Starodubtsev, V.I. Lozinsky, E.V. Kalinina, K. Landfester, A.R. Khohklov, Langmuir 24 (2008) 4467.
[13] D. Ceylan, O. Okay, Macromolecules 40 (2007) 8742.
[14] O. Okay, Prog. Polym. Sci. 25 (2000) 711.
[15] P.J. Flory, Principles of Polymer Chemistry, Cornell University Press, Ithaca, NY, 1953.
[16] L.R.G. Treloar, The Physics of Rubber Elasticity, University Press, Oxford, 1975.
[17] H. Hertz, Über die Berührung Fester Elastischer Körper (on the Contact of Elastic Solids). J. Reineund Angewandte Mathematik 92 (1881) 156, in: D.E. Jones, G.A. Schott (Eds.), Miscellaneous Papers by H. Hertz, Macmillan, London, 1896.
[18] A. Knaebel, S.R. Rebre, F. Lequeux, Polym. Gels. Netw. 5 (1997) 107.
[19] B.J. Briscoe, K.K. Liu, D.R. Williams, J. Coll. Int. Sci. 200 (1998) 256.
[20] M. Barquins, M.E.R. Shanahan, Int. J. Adhes. Adhes. 17 (1997) 313.
[21] W.-M. Lu, K.-L. Tung, S.-M. Hung, J.-S. Shiau, K.-J. Hwang, Powder Technol. 116 (2001) 1.
[22] J. Tiihonen, I. Markkanen, M. Laatikainen, E. Paatero, J. Appl. Polym. Sci. 82 (2001) 256.
[23] M.N. Inci, B. Erman, O. Okay, S. Durmaz, Polymer 42 (2001) 3771.
[24] D. Melekaslan, N. Gundogan, O. Okay, Polym. Bull. 50 (2003) 287.
[25] S. Durmaz, O. Okay, Polymer 41 (2000) 3693.
[26] B.D. Barr-Howell, N.A. Peppas, Eur. Polym. J. 23 (1987) 591.